Received: 7 May 2020 | Accepted: 7 December 2020 | Published: 12 January 2021
DOI:10.20870/oeno-one.2021.55.1.3453

Chemical process to improve natural grapevine-cane extract effectivity against powdery mildew and grey mould

Toni El Khawand, David Taillis, Grégory Da Costa, Eric Pedrot, Stéphanie Cluzet, Alain Decendit, Josep Valls Fonayet and Tristan Richard*

Univ. Bordeaux, ISVV, EA 4577, USC 1366 INRA, Unité de Recherche Œnologie, Molécules d'Intérêt Biologique, 210 chemin de Leysotte, F-33882 Villenave d'Ornon, France

*corresponding author: tristan.richard@u-bordeaux.fr

ABSTRACT

Grapevine canes are vine growing byproducts studied for their antimicrobial activities. These properties are directly connected to the stilbene content; oligomeric stilbenes being the most active. In this study, we propose a chemical process, based on oxidative coupling, using metals to increase the oligostilbene rate and the biological effectivity of cane extract against grapevine pathogens. A total of ten compounds were obtained and identified by combining LCMS and NMR spectroscopies, including four newly reported compounds: *trans*-oxistilbenin C, *trans*-oxistilbenin D, and *cis*- and *trans*-oxistilbenin E. The extract and the main stilbene formed were evaluated for their preventive effects on *Plasmopara viticola* and *Botrytis cinerea* growth. The processed extract was highly effective against both pathogens.

KEYWORDS

resveratrol; viniferin; grapevine; oxidative coupling; *Plasmopara viticola*; *Botrytis cinerea*

Supplementary data can be downloaded through: https://oeno-one.eu/article/view/3453

INTRODUCTION

Stilbenes are a group of polyphenols found in different plant species, especially *Vitis vinifera* (grapevine), and playing the role of phytoalexins (Langcake & Pryce, 1977; Pezet *et al.*, 2004; Rivière *et al.*, 2012). Several studies have already established a link between the attacks of grapevine pathogens and the increase in stilbene production in the plant (Pezet *et al.*, 2003; Vrhovsek *et al.*, 2012). High antimicrobial activity of some stilbenes, especially stilbenes with oligomeric structure (dimers, trimers and tetramers) has been noted (Gabaston *et al.*, 2017; Schnee *et al.*, 2013). Today, there is a growing interest in grapevine stilbenes, which can be sourced from vine growing byproducts, like grapevine canes and roots, for their antimicrobial potential and their likely use for fighting grapevine pathogens like *Plasmopara viticola* and *Botrytis cinerea* (Adrian *et al.*, 1997; Billet *et al.*, 2019; Gabaston *et al.*, 2017; Richard *et al.*, 2016; Schnee *et al.*, 2013). The highest concentrations of resveratrol oligomers are mainly found in extracts of grapevine roots, while grapevine cane extracts show higher concentrations of monomers and dimers, mainly resveratrol and ε-viniferin (Gabaston *et al.*, 2017). However, grapevine canes can be found in larger quantities in comparison with grapevine roots, due to the annual pruning of the plant.

Several studies showed that oxidative coupling of resveratrol was possible using metals (Sako *et al.*, 2004; Snyder *et al.*, 2011; Velu *et al.*, 2008) leading to the formation of effective compounds against grapevine pathogens (El Khawand *et al.*, 2020a). These reactions could take place in different media including wine (El Khawand *et al.*, 2020b). Hence, the hemisynthesis of resveratrol oligomers using resveratrol and ε-viniferin found in large amounts in cane extracts could be an efficient and fast way to produce an enriched stilbene extract, with high antimicrobial activity.

The original purpose of this study was to use oxidative coupling to produce a more active extract from a natural source rich in resveratrol and ε-viniferin. Oxidative coupling using silver acetate was directly applied on a grapevine-cane fraction with high content in resveratrol and ε-viniferin. Main compounds of the reaction mixture were isolated and identified by spectroscopic analysis (UHPLC–MS, 1D- and 2D-NMR) including new reported active resveratrol oligomers. Biological activities were evaluated *in vitro* on downy mildew (*Plasmopara viticola*) and grey mould diseases (*Botrytis cinerea*), two of the most common grapevine diseases.

MATERIALS AND METHODS

1. Chemicals

All reagents were of analytical grade and used as received without further purification. Methanol (HPLC grade), ethanol (HPLC grade), acetonitrile (HPLC and LC-MS grades, purity ≥ 99.9 %), ethyl acetate (laboratory reagent grade) and formic acid were purchased from Fisher Scientific (Loughborough, United Kingdom). Ethyl acetate (HPLC grade), potato dextrose broth and agar were purchased from Sigma-Aldrich (Saint-Louis, USA). *n*-Heptane (HPLC grade) was purchased from VWR International (Fontenay-sous-Bois, France). Silver acetate (purity ≥ 99 %) was purchased from Acros organics (Geel, Belgium). Ultrapure water (8 MΩ.cm) was obtained from an Elga apparatus (High Wycombe, United Kingdom).

2. Cane extract and CPC fractionation

Grapevine cane extract was kindly provided by Actichem (Montauban, France) produced using a mixture of Cabernet Sauvignon and Merlot cultivars grown in the Bordeaux region (France). The stilbene composition of the cane extract was previously described (Müller *et al.*, 2009; Romain *et al.*, 2014). To obtain a purified extract with high stilbene content, fractionation was performed using centrifugal partition chromatography (CPC) according to a previously published protocol (Biais *et al.*, 2017). Briefly, the CPC was realized on a Kromaton FCPC® 1000 apparatus (Angers, France) equipped with an Iota S100 pump, a Flash 06 DAD 600 detector and a Spider mixing unit manufactured by Ecom (Prague, Czech Republic). Fractionation was achieved using the K Arizona biphasic solvent system composed of *n*-heptane/ethyl acetate/MeOH/H_2O (1/2/1/2, v/v). The fraction richest in resveratrol and εviniferin was collected. This purified extract contained mainly resveratrol, εviniferin and rviniferin (320, 570, and 60 mg/g, respectively) (Biais *et al.*, 2017).

3. Oxidative coupling reaction

Based on our previously published protocol (El Khawand *et al.*, 2020a), regioselective oxidative coupling reaction was conducted on 1 g of the purified extract. The quantity of the

silver acetate (AgOAc) metallic catalyst added to perform the reaction was calculated according to the quantities of resveratrol and εviniferin in the extract, to afford a stilbene:AgOAc ratio of 1:1.5 The purified extract and AgOAc were dissolved in MeOH (100 %, 100 mL). The reaction mixture turned to an ash colour as it was heated at 50 °C and stirred for 2 hours. The reaction was then stopped by cooling at 4°C and centrifuged. The MeOH fraction was collected and the solvent was removed under reduced pressure. Finally, the grapevine cane processed extract (GCPE) was lyophilized.

4. UHPLC analysis

Extracts were analyzed on a UHPLC-DAD-IT-MS Agilent 1290 series apparatus (Santa Clara, Canada) equipped with an autosampler module, a binary pump, a degasser, a column heater/ selector, a UV-VIS-DAD, and an Ion Trap (Esquire 6000, Bruker-Daltonics, Billerica, MA). The elution was performed on an Agilent SB-C18 (2.1 mm × 100 mm, 1.8 µm) column at a flow rate of 0.4 mL/min, with acidified water (0.1 % formic acid, solvent A) and acidified acetonitrile (0.1 % formic acid, solvent B) according to the following gradient: 10 % B (0.0–1.7 min), 10–20 % B (1.7–3.4 min), 20–30 % B (3.4–5.1 min), 30 % B (5.1–6.8 min), 30–35 % B (6.8–8.5 min), 35–60 % B (8.5–11.9 min), 60–100 % B (11.9−15.3 min), 100 % B (15.3–17.0 min), 100-10 % B (17–17.30 min). The MS method was conducted in negative mode, scan range: m/z 130–1200, drying gas: 10 L/min, nebulizer pressure: 40 psi, temperature: 365°, capillary voltage: 4000 V, capillary exit voltage: −108 V, skimmer voltage: −40 V, trap drive: 47.1. Samples were injected at a concentration of 100 µg/mL after solubilization in H_2O/MeOH mixture (1:1, v/v).

5. Isolation and identification of the reaction products

Stilbenes were purified from GCPE extract using preparative HPLC. The apparatus was a Gilson PLC 2050 system (Middleton, WI, USA) equipped with a UV-VIS detector. Elution was conducted on a Phenomenex Kinetex XB-C18 column (21.2 mm × 250 mm, 5 µm). The reaction extract powder was solubilized at 50 mg/mL in MeOH-H_2O (50/50; v/v). The extract was then eluted with a flow rate of 20 mL/min using non-acidified ultrapure water (solvent A) and acetonitrile (solvent B), according to the following gradient: 33 % B (0–2 min), 33–50 % B (2–25 min), 50–100 % B (25–26 min) and 100 % B (26–31 min). The eluate was monitored at 280 and 306 nm and the fractions were automatically collected. Syringes were purchased from Millipore (Molsheim, France). The solvents were removed under reduced pressure and fractions were lyophilized.

The pure compounds were analyzed using UHPLC as previously described and their purity was estimated to be ≥ 90 %. Exact masses were determined by infusion on a Thermo Fisher Exactive Plus Orbitrap mass spectrometer (Waltham, Massachusetts, USA) in negative mode with the following parameters: full scan mode, scan range 100–800 m/z, resolution 280,000, automatic gain control (AGC) target value of 2E5, maximum ion injection time (IT) of 30 ms; H-ESI source parameters: spray voltage 2700 V, sheath gas flow rate 8, capillary temperature 320 °C. The structures of purified compounds were finally determined by 1D- and 2D-experiments including COSY, HSQC, HMBC and ROESY, using a Bruker Avance III 600 NMR spectrometer (Rheinstetten, Germany).

6. Bioassays

6.1. *Plasmopara viticola* development inhibition

Grapevine leaves (*Vitis vinifera* L., Cabernet-Sauvignon cultivar) were collected from the upper part of the shoots from plants produced by wood-cutting propagation and grown in the INRA nursery (Villenave d'Ornon, France), under controlled conditions of temperature (25/20 °C, day/night) and humidity (75 %) with a photoperiod of 16/8 hours (light/dark). The *P. viticola* isolate ANN-01 used in the assay was collected in 2015 from Ugni Blanc grapevine cultivar leaves in a commercial vineyard (Charente, France). To obtain the required quantity of pathogen material, an inoculum (sporangia suspension) of *P. viticola* was taken from spores stored at –20°C, and grown on Cabernet Sauvignon leaves for 7 days, before proceeding to the development inhibition assay. This multiplication step was followed by the inhibition assay. Leaf disks were cut from Cabernet Sauvignon fresh leaves, treated with the stilbene solutions prepared in sterile water with 1 % of ethanol, and then by an aqueous suspension of 20,000 sporangia/mL as described in a previous study (Gabaston*et al.*, 2017). According to previous works, and by monitoring the development of the pathogen on the control leaf disks treated with water/ethanol (99/1, v/v), it should be noted that one percent of ethanol

in water does not affect zoospore mobility and disease development (Pezet *et al.*, 2004).

6.2. *Botrytis cinerea* mycelium development inhibition

This in vitro assay was similar to that used by Adrian *et al.* (1997). The culture medium was a mixture of potato dextrose broth (24 g/L) and agar (15 g/L), autoclaved at 120 °C for 20 min. Ethanol solutions of the evaluated compounds were prepared at the concentrations of 0.5, 1, 2, 5, 10, 20 and 50 mg/mL. The compound solutions were then incorporated in the autoclaved culture medium (240 µL/12 mL, solution/medium) to obtain final concentrations of 5, 10, 20, 50, 100, 200 and 500 mg/L with 2 % ethanol. Dishes of 6 wells were used and each mixture was poured in 3 wells, 4 mL/well. A calibrated plug of mycelium of *B. cinerea* was then inoculated on the culture medium, and the dishes were incubated at 22 °C, with a photoperiod of 15/9 hours (light/dark). Measurements of the mycelium growth area were performed after 48 h and 60 h of incubation, leading to the calculation of the inhibition rate according to each concentration of the tested compounds and extracts, and hence determining IC_{50} for each tested compound or extract.

7. Statistical Analyses

Three independent experiments of eight repetitions were carried out for each assay. Data are shown as means ± SEM. The statistical analysis was performed on the three extracts at each specific concentration. One-way ANOVA with post-hoc Tukey HSD tests was carried out. Significant differences between each extract were set at $^{**}p < 0.01$ and $^{*}p < 0.05$.

RESULTS AND DISCUSSION

1. Production and analysis of the grapevine cane processed extract

The purpose of this study is to directly apply an oxidative coupling strategy directly on a stilbene enriched extract obtained from grapevine canes to increase the extract antimicrobial activity. Since cane extract contains several different compounds with no more than 45% of stilbenes (Müller *et al.*, 2009; Romain *et al.*, 2014), the extract was firstly fractionated by centrifugal partition chromatography (CPC) following a procedure previously published (Biais *et al.*, 2017). The fraction containing the main stilbenes of the cane extract was collected to proceed to the oxidative coupling using silver acetate (AgOAc). The UPLC-DAD-MS chromatogram of this fraction is presented in Figure 1A. The fraction contained three main stilbenes (see Figure S1 for chemical structure): *trans*-resveratrol, *trans*-ε-viniferin, and r-viniferin (320, 570, and 60 mg/g, respectively). In addition, minor compounds could be present such as miyabenol C, ωviniferin and δviniferin (Biais *et al.*, 2017).

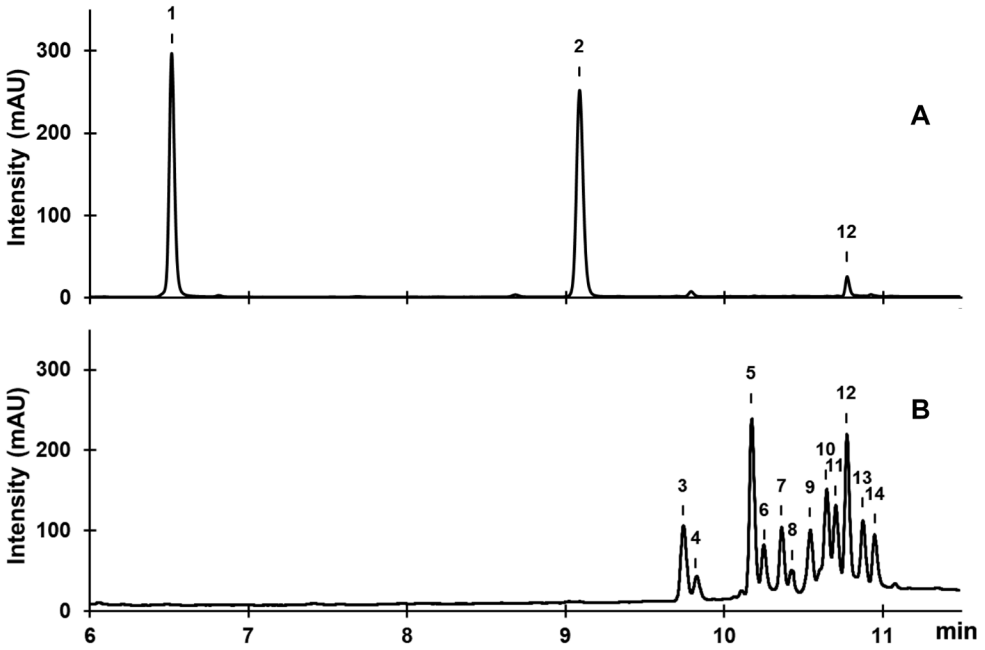

FIGURE 1. Ultra-high-performance liquid chromatographic-diode array (UHPLC-DAD) chromatograms. (A) initial cane fraction, and (B) grapevine cane processed extract (GCPE) extract measured at 280 nm.

TABLE 1. GCPE extract compounds. Peak number, retention time, compound name, MS data and amount.

N°	t_R (min)	Compound name	$[M - H]^-$	Amount (mg/g)
3	9.74	*trans*-oxistilbenin A	485	40
4	9.82	*trans*-oxistilbenin B	485	30
5	10.17	*trans*-δ-viniferin	453	140
6	10.20	unknown	679	10
7	10.36	*trans*-oxistilbenin C	679	60
8	10.42	*trans*-resviniferin A + *cis*-resviniferin A	679	20
9	10.54	*trans*-oxistilbenin D	711	50
10	10.65	*cis*-oxistilbenin E	679	130
11	10.70	*trans*-oxistilbenin E	679	60
12	10.77	r-viniferin	905	140
13	10.87	unknown	905	90
14	10.95	unknown	905	40

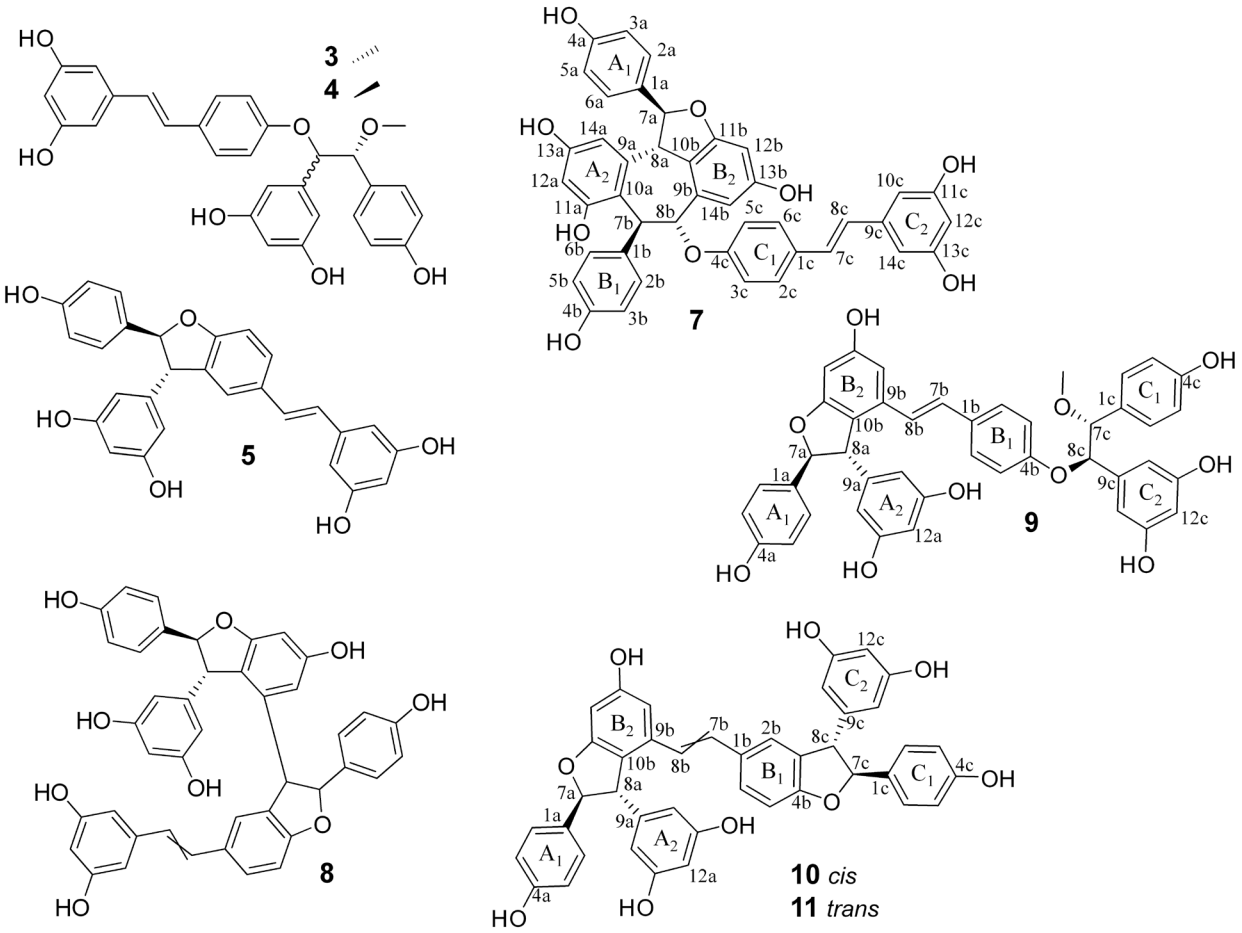

FIGURE 2. Structure of the newly produced compounds after oxidative coupling.

The UPLC-DAD-MS chromatogram of the grapevine-cane extract (GCPE) obtained after oxidative coupling by AgOAc is presented in Figure 1B. The lyophilization of the reaction mixture led to a dark brown soft powder. The analysis of the chromatogram indicates the formation of at least eleven compounds, and shows that under stirring condition, 100 % of resveratrol and ε-viniferin reacted. The r-viniferin probably did not react but increased due to the oligomerization of εviniferin (Sako *et al.*, 2004). The total transformation of resveratrol and ε-viniferin was achieved using a molar ratio 1:1.5 (stilbene:AcOAg).

To identify the *de novo* synthetized compounds, the extract was further purified using reversed-phase chromatography. This technique allowed us to collect twelve fractions containing from 20 to 140 mg of stilbene oligomers, for a total of 810 mg/g (Table 1). Based on their molecular masses, stilbene oligomers were detected including dimers (peaks **3**, **4** and **5**), trimers (peaks **6**, **7**, **8**, **9**, **10** and **11**), and tetramers (peaks **12**, **13** and **14**). The structures of the isolated compounds were elucidated by NMR spectroscopy. A total of 10 compounds were identified (Table 1 and Figure 2). In addition to the previously reported *trans*-oxistilbenin A and B (**3** and **4**, respectively) (El Khawand *et al.*, 2020a), *trans*-δ-viniferin (**5**) (Takaya *et al.*, 2005), *trans*- and *cis*-resviniferin A (**8**) (Wilkens*xet al.*, 2010), and r-viniferin (**12**) (Takaya*et al.*, 2002b), four newly reported stilbenes were identified as *trans*-oxistilbenin C (**7**), *trans*-oxistilbenin D (**9**), *cis*- and *trans*-oxistilbenin E (**10** and **11**, respectively).

The structures of the identified compounds were obtained by mass spectrometry analysis and NMR spectroscopy, including 2D experiments such as COSY, ROESY, HSQC, and HMBC.

The *trans*-oxistilbenin C (**7**) was obtained as a pale brown amorphous powder, with a high-resolution molecular ion in negative mode at *m/z* 679.1942 $[M - H]^-$ corresponding to a resveratrol trimer. The NMR data of **7** are reported in Table 2. The ^{1}H-NMR spectrum exhibited three sets of AA'XX' type ortho-coupled aromatic protons at δ 6.79 and 7.15 (2H each, d, J = 8.7 Hz) for ring A_1, 6.68 and 6.99 (2H each, d, J = 8.7 Hz) for ring B_1, 7.07 and 7.51 (2H each, d, J = 8.7 Hz) for ring C_1, two sets of meta-coupled aromatic protons at δ 6.27 (1H, d, J = 2.0 Hz) and 6.36 (1H, brs) for ring A_2, 6.22 and 6.54 (1H each, d, J = 2.1 Hz) for ring B_2, one set of AX2 type meta-coupled aromatic protons at δ 6.57 (2H, d, J = 2.1 Hz) and 6.28 (1H, t, J = 2.1 Hz) for ring C_2, two coupled doublets at δ 6.94 and 7.07 (1H each, d, J = 16.2 Hz) for a *trans*-configured double bond, and two sets of mutually coupled aliphatic methine protons at δ 4.24 and 5.85 (1H each, d, J = 11.3 Hz), 5.74 and 6.25 (1H each, d, J = 4.7 Hz). The correlations of the aromatic rings, double bonds and aliphatic protons were deduced from the COSY spectrum. All the protonated carbons were identified from the HSQC spectrum. The structure of **7** was proposed after examination of the CH long-range correlations from the HMBC spectrum (Figure S2). The correlations of proton H-8a (δ 4.24) with eight carbon signals [δ 130.3 (C-1a), 87.7 (C-7a), 141.7 (C-9a), 117.5 (C-10a), 104.5 (C-14a), 136.1 (C-9b), 118.9 (C-10b), 158.0 (C-11b)] and proton H-7b (δ 5.74) with seven carbon signals [δ 141.7 (C-9a), 117.5 (C-10a), 157.8 (C-11a), 131.0 (C-1b), 128.0 (C-2b), 77.2 (C-8b), 136.1 (C-9b)] indicated the connectivity between the monomers units A and B. The correlations between proton H-8b (δ 6.25) and carbon C-4c (δ 159.2) provided the connection between monomer unit B and aromatic ring C_1. The relative stereochemistry of protons H-7a, H-8a, H-7b and H-8b was deduced from the ROESY spectrum and comparison with literature data (Oshima *et al.*, 1990; Takaya *et al.*, 2002a). The NOE correlations H-8a / H-2a(6a) and H7a / H14a indicated the *trans* orientation of the two methine protons of the dihydrobenzofuran moiety. The correlation between H-2b(6b) / H-8a suggests that the C-7b aryl group is situated *cis* to H8a. Finally, the α-configuration of the monomer unit C on C-8b was indicated by the NOE correlations H-7b / H-2c(6c) and H-8b / H-2b(6b).

The *trans*-oxistilbenin D (**9**) was obtained as a pale brown amorphous powder, with a high-resolution molecular ion in negative mode at *m/z* 711.2203 $[M - H]^-$ corresponding to an *O*-methylated resveratrol trimer. The NMR data of **9** are reported in Table 2. The ^{1}H-NMR spectrum exhibited three sets of AA'XX' type ortho-coupled aromatic protons at δ 6.83 and 7.20 (2H each, d, J = 8.7 Hz) for ring A_1, 6.79 and 7.15 (2H each, d, J = 8.7 Hz) for ring B_1, 6.70 and 7.03 (2H each, d, J = 8.7 Hz) for ring C_1, one set of meta-coupled aromatic protons at δ 6.31 (1H, d, J = 2.1 Hz) and 6.70 (1H, d, J = 2.1 Hz) for ring B_2, two sets of AX2 type meta-coupled aromatic protons at δ 6.20 (2H, brs) and 6.21 (1H, brs) for ring A_2, 6.18 (2H, d, J = 2.1 Hz) and 6.13 (1H, t, J = 2.1 Hz) for ring C_2, two coupled doublets at δ 6.88 and 6.70 (1H each, d, J = 16.6 Hz) for a *trans*-configured double bond, two sets of mutually coupled aliphatic

TABLE 2. NMR data of compounds 7, 9, 10 and 11 in acetone-d_6.

	7		**9**		**10**		**11**	
	δ_C	δ_H (mult., *J* in Hz)	δ_C	δ_H (mult., *J* in Hz)	δ_C	δ_H (mult, *J* in Hz)	δ_C	δ_H (mult, *J* in Hz)
1a	130.3	-	133.1	-	131.6	-	131.0	-
2a	129.1	7.15 (d, 8.7)	127.2	7.20 (d, 8.7)	127.6	7.21 (d, 8.6)	127.9	7.23 (d, 8.6)
3a	115.2	6.79 (d, 8.7)	115.2	6.83 (d, 8.7)	115.3	6.85 (d, 8.6)	115.2	6.87 (d, 8.6)
4a	157.7	-	157.2	-	157.4	-	157.7	-
5a	115.2	6.79 (d, 8.7)	115.2	6.83 (d, 8.7)	115.3	6.85 (d, 8.6)	115.2	6.87 (d, 8.6)
6a	129.1	7.15 (d, 8.7)	127.2	7.20 (d, 8.7)	127.6	7.21 (d, 8.6)	127.9	7.23 (d, 8.6)
7a	87.7	5.85 (d, 11.3)	93.0	5.40 (d, 5.3)	93.1	5.38 (d, 8.6)	93.2	5.32 (d, 9.3)
8a	48.8	4.24 (d, 11.3)	56.1	4.46 (d, 5.3)	56.9	4.33 (d, 8.6)	57.0	4.40 (d, 9.3)
9a	141.7	-	146.6	-	143.7	-	143.5	-
10a	117.5	-	106.2	6.20 (brs)	106.6	6.12 (d, 2.2)	106.7	6.11 (d, 2.2)
11a	157.8	-	159.0	-	158.8	-	158.8	-
12a	102.7	6.36 (brs)	101.2	6.21 (brs)	101.7	6.24 (t, 2.2)	101.9	6.26 (t, 2.2)
13a	156.5	-	159.0	-	158.8	-	158.8	-
14a	104.5	6.27 (d, 2.0)	106.2	6.20 (brs)	106.6	6.12 (d, 2.2)	106.7	6.11 (d, 2.2)
1b	131.0	-	135.2	-	130.2	-	129.7	-
2b	128.0	6.99 (d, 8.7)	127.5	7.15 (d, 8.7)	126.3	6.82 (d, 1.9)	125.8	6.79 (d, brs)
3b	114.8	6.68 (d, 8.7)	114.8	6.79 (d, 8.7)	132.8	-	132.8	-
4b	155.5	-	158.3	-	161.4	-	161.2	-
5b	114.8	6.68 (d, 8.7)	114.8	6.70 (d, 8.7)	128.9	7.07 (dd, 1.9, 8.3)	128.3	7.03 (dd, 1.7, 8.3)
6b	128.0	6.99 (d, 8.7)	127.5	7.15 (d, 8.7)	108.8	6.68 (d, 8.3)	108.8	6.64 (d, 8.3)
7b	39.2	5.74 (d, 4.7)	128.9	6.88 (d, 16.6)	130.4	6.26 (d, 11.9)	128.3	6.96 (d, 16.3)
8b	77.2	6.25 (d, 4.7)	123.3	6.70 (d, 16.6)	125.7	6.03 (d, 11.9)	126.8	6.86 (d, 16.3)
9b	136.1	-	133.5	-	136.1	-	135.9	-
10b	118.9	-	119.0	-	119.3	-	119.4	-
11b	158.0	-	161.6	-	161.6	-	161.7	-
12b	96.9	6.22 (d, 2.1)	95.9	6.31 (d, 2.1)	95.8	6.30 (d, 2.2)	95.9	6.31 (d, 2.2)
13b	159.7	-	158.7	-	158.4	-	158.7	-
14b	109.7	6.54 (d, 2.1)	103.3	6.70 (d, 2.1)	106.7	6.33 (d, 2.2)	107.7	6.32 (d, 2.2)
1c	130.2	-	129.3	-	131.5	-	133.0	-
2c	127.6	7.51 (d, 8.7)	129.4	7.03 (d, 8.7)	127.3	7.09 (d, 8.6)	127.9	7.06 (d, 8.6)
3c	116.4	7.07 (d, 8.7)	114.7	6.70 (d, 8.7)	115.1	6.82 (d, 8.6)	115.2	6.87 (d, 8.6)
4c	159.2	-	156.9	-	157.4	-	157.3	-
5c	116.4	7.07 (d, 8.7)	114.7	6.70 (d, 8.7)	115.1	6.82 (d, 8.6)	115.2	6.87 (d, 8.6)
6c	127.6	7.51 (d, 8.7)	129.4	7.03 (d, 8.7)	127.3	7.09 (d, 8.6)	127.9	7.06 (d, 8.6)
7c	128.8	7.07 (d, 16.2)	86.9	4.42 (d, 6.6)	93.3	5.29 (d, 5.6)	93.3	5.29 (d, 5.3)
8c	126.5	6.94 (d, 16.2)	83.4	5.15 (d, 6.6)	56.1	4.04 (d, 5.6)	56.1	3.96 (d, 5.3)
9c	140.0	-	140.7	-	146.1	-	146.1	-
10c	104.9	6.57 (d, 2.1)	106.2	6.18 (d, 2.1)	106.2	6.04 (d, 2.2)	106.2	6.05 (d, 2.2)
11c	158.8	-	158.0	-	158.8	-	158.8	-
12c	101.9	6.28 (t, 2.1)	101.8	6.13 (t, 2.1)	101.0	6.19 (t, 2.2)	101.1	6.20 (t, 2.2)
13c	158.8	-	158.0	-	158.8	-	158.8	-
14c	104.9	6.57 (d, 2.1)	106.2	6.18 (d, 2.1)	106.2	6.04 (d, 2.2)	106.2	6.05 (d, 2.2)
OMe			56.3	3.20 (s)				

methine protons at δ 4.46 and 5.40 (1H each, d, *J* = 5.3 Hz), 4.42 and 5.15 (1H each, d, *J* = 6.6 Hz), and one O-methyl group at δ 3.20 (3H, s). The correlations of the aromatic rings, double bonds and aliphatic protons were obtained from the COSY spectrum. All the protonated carbons were identified from the HSQC spectrum. The structure of **9** was proposed after an examination of the CH long-range correlations from the HMBC spectrum (Figure S3). The correlations of proton H-8a (δ 4.46) with seven carbon signals [δ 133.1 (C-1a), 93.0 (C-7a), 146.6 (C-9a), 106.2 (C-10a(14a)), 133.5 (C-9b), 119.0 (C-10b), 161.6 (C-11b)] indicated the connectivity between the monomer unit A and aromatic ring B_2. The correlations between proton H-8c (δ 5.15) with five carbon signals [δ 158.3 (C-4b), 129.3 (C-1c), 86.9 (C-7c), 140.7 (C-9c), 106.8 (C-10c(14c))] provided the connection between monomer unit C and aromatic ring B_1. The relative stereochemistry of protons H-7a, H-8a, H-7c and H-8c was deduced from ROESY spectrum and comparison with literature data (Oshima *et al.*, 1990; Takaya *et al.*, 2002a). The NOE correlations H-8a / H-2a(6a) and H7a / H10a(14a) indicated the *trans* orientation of the two methine protons of the dihydrobenzofuran moiety. The correlations between H-2c(6c) / H-8c and H-10c(14c) / H-7c suggest that the C-7c aryl group is situated *cis* to H8c.

The *cis*-oxistilbenin E (**10**) was obtained as a pale brown amorphous powder, with a high-resolution molecular ion in negative mode at *m/z* 679.1944 $[M - H]^-$ corresponding to a resveratrol trimer. The NMR data of **10** are reported in Table 2. The ^{1}H-NMR spectrum exhibited two sets of AA'XX' type ortho-coupled aromatic protons at δ 6.85 and 7.21 (2H each, d, *J* = 8.6 Hz) for ring A_1, 6.82 and 7.09 (2H each, d, *J* = 8.6 Hz) for ring C_1, one set of meta-coupled aromatic protons at δ 6.30 (1H, d, *J* = 2.2 Hz) and 6.33 (1H, d, *J* = 2.2 Hz) for ring B_2, two sets of AX2 type meta-coupled aromatic protons at δ 6.12 (2H, d, *J* = 2.2 Hz) and 6.24 (1H, t, *J* = 2.2 Hz) for ring A_2, 6.04 (2H, d, *J* = 2.2 Hz) and 6.19 (1H, t, *J* = 2.2 Hz) for ring C_2, one set of ABX type ortho-meta-coupled aromatic protons at δ 6.68 (1H, d, *J* = 8.3 Hz), 6.82 (1H, d, *J* = 1.9 Hz) and 7.07 (1H, dd, *J* = 1.9 and 8.3 Hz) for ring B_1, two coupled doublets at δ 6.26 and 6.03 (1H each, d, J = 11.9 Hz) for a *cis*- configured double bond, and two sets of mutually coupled aliphatic methine protons at δ 4.33 and 5.38 (1H each, d, *J* = 8.6 Hz), 4.04 and 5.29 (1H each, d, *J* = 5.6 Hz). The correlations of the aromatic rings, double bonds and aliphatic protons were obtained from the COSY spectrum. All the protonated carbons were identified from the HSQC spectrum. The structure of **10** was proposed after an examination of the CH long-range correlations from the HMBC spectrum (Figure S4). The correlations of proton H-8a (δ 4.33) with seven carbon signals [δ 131.6 (C-1a), 93.1 (C-7a), 143.7 (C-9a), 106.6 (C-10a(14a)), 136.1 (C-9b), 119.3 (C-10b), 161.6 (C-11b)] indicated the connectivity between the monomer unit A and aromatic ring B_2. The correlations between proton H-8c (δ 4.04) with seven carbon signals [δ 131.5 (C-1c), 93.3 (C-7c), 146.1 (C-9c), 106.2 (C-10c(14c)), 126.3 (C-2b), 132.8 (C-3b), 161.4 (C-4b)] indicated the connectivity between the monomer unit C and aromatic ring B_1. The relative stereochemistry of protons H-7a, H-8a, H-7c and H-8c was deduced from the ROESY spectrum. The NOE correlations H-8a / H-2a(6a) and H8c / H-2c(6c) indicate, respectively, the *trans* orientation of the methine protons of the two dihydrobenzofuran moieties.

The *trans*-oxistilbenin E (**11**) was obtained as a pale brown amorphous powder, with a high-resolution molecular ion in negative mode at *m/z* 679.1944 $[M - H]^-$ corresponding to a resveratrol trimer. NMR data of compound **11** are very similar to **10** (Table 2) except for the two coupled doublets at δ 6.86 and 6.96 (1H each, d, J = 16.3 Hz) that indicated the presence of a *trans*- configured double bond.

The compounds identified in this study were formed by oxidative reactions between resveratrol and ε-viniferin moieties. The structures observed suggest that reactions take place on the 4-OH positions of the stilbenes (Takaya *et al.*, 2005; Takaya *et al.*, 2002b). The coupling between two resveratrol moieties leads to the formation of compounds **3**, **4**, and **5** (Figure 5S). The reaction between resveratrol and ε-viniferin induces the formation of compounds **7**, **8** and **9-11** (Figure 6S). Finally, the oxidative coupling between two ε-viniferin units leads to the formation of compound **12** (Figure 7S).

2. Antimicrobial activities

2.1. Antimicrobial activity against *Plasmopara viticola*

Grapevine extract effectiveness against downy mildew has been demonstrated *in vitro* (Gabaston *et al.*, 2017; Schnee *et al.*, 2013) in greenhouse and vineyard (Richard *et al.*, 2016). In this study, grapevine leaves were treated with the grapevine-cane extract obtained after oxidative

coupling by AgOAc (GCPE extract). The results were compared to the effects of the initial grapevine-cane extract (Figure 3A). GCPE extract gave a total inhibition for concentrations upper to 200 mg/L, whereas the same effect was observed for the CE extract from 500 mg/L. The chemically engineered extract was three times more active than the initial extract against downy mildew (IC_{50} 63 ± 9 mg/L and 197 ± 12 mg/L, respectively). This process induced the production of a more active solution than the initial grapevine extract. This solution could be used to reduce the application rates by maximizing the effectiveness of treatments.

In addition, the antimicrobial activities of the isolated compounds were evaluated. The IC_{50} of the main stilbenes isolated and identified were reported in Table 3. Resveratrol was used as standard and the resulting IC_{50} value agreed with literature data (Gabaston *et al.*, 2017; Schnee *et al.*, 2013). The highest activity against *P. viticola* growth, and thus the lowest IC_{50} values, was obtained for rviniferin (14 µM) followed by a pool of *de novo* synthetized compounds including δ-viniferin (40 µM), *trans*- and *cis*-oxistilbenin E (31 and 34 µM, respectively), and *trans*-oxistilbenin B (44 µM). As previously reported (Gabaston *et al.*, 2017; Schnee *et al.*, 2013), we observed a positive correlation between the degree of oligomerization and the inhibition of the development of pathogens.

2.2. Antimicrobial activity against *Botrytis cinerea*

Fungitoxicity of extracts and pure compounds were monitored using radial growth test. *B. cinerea* growth areas were measured to calculate the inhibition rate according to each concentration of the tested compounds and extracts, and hence determining IC_{50}. Firstly, Efficacy of the GCPE extract was compared to that of initial grapevine-cane extract (Figure 3B). The grapevine cane extract exhibited a moderate effect against the development of *B. cinerea*. This finding is in agreement with the literature (Schnee *et al.*, 2013). Cane extract is less effective against the grey mould agent. In contrast, the GCPE extract was more effective reaching 100 % inhibition at 100 mg/L and exhibiting an IC_{50} of 5 ± 9 mg/L.

The IC_{50} of the pure constituents of the GCPE extract are shown in Table 3. As previously reported (Gabaston *et al.*, 2017), resveratrol presented a moderate antifungal activity (IC_{50} 430 µM). The rviniferin was the most active inhibitor of *B. cinerea* development, presenting the lowest IC_{50} 9 µM, followed by δ-viniferin (13 µM) and resviniferin A (27 µM). The oxidative coupling induced the production of an active pool of stilbene oligomers against *B. cinerea* development. The process could be useful to increase the efficacy of canes to prevent grapevine diseases. The GCPE extract could maximize the effectiveness of treatments; reduce the application rates and the number of interventions.

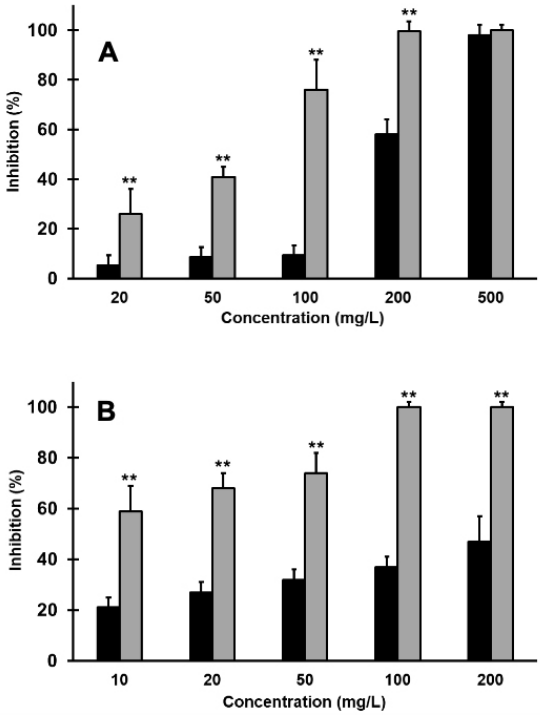

FIGURE 3. Comparison of the preventive effects *P. viticola* development (A), and *B. cinerea* mycelial growth (B). Grapevine cane and GCPE extracts in black and grey, respectively. Results are expressed as means ± SEM.

TABLE 3. IC_{50} values (µM) of identified compounds against *P. viticola* and *B. cinerea*.

	P. viticola	*B. cinerea*
	IC_{50}	IC_{50}
resveratrol	434 ± 39	430 ± 44
trans-oxistilbenin A (**3**)	130 ± 25	128 ± 6
trans-oxistilbenin B (**4**)	44 ± 11	57 ± 7
δ-viniferin **(5)**	40 ± 7	13 ± 4
trans-oxistilbenin C **(7)**	53 ± 13	134 ± 18
resviniferin A **(8)**	60 ± 13	27 ± 10
trans-oxistilbenin D **(9)**	93 ± 11	104 ± 15
cis-oxistilbenin E **(10)**	34 ± 7	31 ± 15
trans-oxistilbenin E **(11)**	31 ± 6	34 ± 15
r-viniferin **(12)**	14 ± 5	9 ± 6

[a] concentration expressed in µM. nd: not determined

CONCLUSION

First, at all, we have developed an original approach to produce an active product from a natural vine extract. Findings in this study confirmed that oligomeric stilbenes have strong antimicrobial activity against grapevine pathogens. This study confirmed a positive correlation between the degree of oligomerization and the inhibition of pathogen development. The protocol induced the hemisynthesis of a pool of oligomeric stilbenes including r-viniferin, δ-viniferin, and the newly reported *trans*-oxistilbenin C, *trans*-oxistilbenin D, *cis*- and *trans*-oxistilbenin E. The initial grapevine extract was more active on *P. viticola* than on *B. cinerea* development. Its low efficiency against grey mould agent precludes its use in the field due to the large amount of canes necessary to produce this active product. The GCPE extract produced by oxidative coupling had the highest antimicrobial activity against *P. viticola* and *B. cinerea*. Interestingly, this extract strongly inhibited both grapevine pathogens. The use of this process could be a solution to reduce the doses necessary to treat downy mildew and to prevent the effects of gray mold in grapevine. To confirm the interest of this innovative approach, greenhouse and field trials will have to be carried out.

ACKNOWLEDGEMENTS

The authors gratefully thank Actichem (Montauban, France) for providing grapevine products and Marie-France Corio-Costet (UMR 1065 SAVE, INRAe) to provide us the plant and fungal materials for the antimicrobial assays. The work was supported by the Bordeaux Metabolome Facility and MetaboHUB (ANR-11- INBS-0010 project).

REFERENCES

Adrian, M., Jeandet, P., Veneau, J., A. Weston, L., & Bessis, R. (1997). Biological activity of resveratrol, a stilbenic compound from grapevines, against *Botrytis cinerea*, the causal agent for gray mold. *Journal of Chemical Ecology, 23*, 1689-1702. doi:10.1023/B:JOEC.0000006444.79951.75

Biais, B., Krisa, S., Cluzet, S., Da Costa, G., Waffo-Teguo, P., Mérillon, J. M., & Richard, T. (2017). Antioxidant and cytoprotective activities of grapevine stilbenes. *Journal of Agricultural and Food Chemistry, 65*(24), 4952-4960. doi:10.1021/acs.jafc.7b01254

Billet, K., Delanoue, G., Arnault, I., Besseau, S., Oudin, A., Courdavault, V., Marchand, P. A., Giglioli-Guivarc'h, N., Guérin, L., & Lanoue, A. (2019). Vineyard evaluation of stilbenoid-rich grape cane extracts against downy mildew: a large-scale study. *Pest Management Science, 75*(5), 1252-1257. doi:10.1002/ps.5237

El Khawand, T., Gabaston, J., Taillis, D., Iglesias, M.-L., Pedrot, E., Palos Pinto, A., Valls Fonayet, J., Merillon, J. M., Decendit, A., Cluzet, S., & Richard, T. (2020a). A dimeric stilbene extract produced by oxidative coupling of resveratrol active against *Plasmopara viticola* and *Botrytis cinerea* for vine treatments. *OENO One, 54*(1), 157-164. doi:10.20870/oeno-one.2020.54.1.2529

El Khawand, T., Valls Fonayet, J., Da Costa, G., Hornedo-Ortega, R., Jourdes, M., Franc, C., de Revel, G., Decendit, A., Krisa, S., & Richard, T. (2020b). Resveratrol transformation in red wine after heat treatment. *Food Research International, 132*. doi:10.1016/j.foodres.2020.109068

Gabaston, J., Cantos-Villar, E., Biais, B., Waffo-Teguo, P., Renouf, E., Corio-Costet, M.-F., Richard, T., & Mérillon, J.-M. (2017). Stilbenes from *Vitis vinifera* L. waste: a sustainable tool for controlling *Plasmopara viticola*. *Journal of Agricultural and Food Chemistry, 65*(13), 2711-2718. doi:10.1021/acs.jafc.7b00241

Langcake, P., & Pryce, R. J. (1977). A new class of phytoalexins from grapevines. *Experientia, 33*(2), 151-152. doi:10.1007/bf02124034

Müller, C., Ullmann, K., Wilkens, A., Winterhalter, P., Toyokuni, S., & Steinberg, P. (2009). Potent antioxidative activity of vineatrol®30 grapevine-shoot extract. *Bioscience, Biotechnology, and Biochemistry, 73*(8), 1831-1836. doi:10.1271/bbb.90213

Oshima, Y., Ueno, Y., Hikino, H., Ling-Ling, Y., & Kun-Ying, Y. (1990). Ampelopsins A, B and C, new oligostilbenes of *Ampelopsis brevipedunculata* VAR. Hancei. *Tetrahedron, 46*(15), 5121-5126. doi:10.1016/S0040-4020(01)87819-4

Pezet, R., Gindro, K., Viret, O., & Richter, H. (2004). Effects of resveratrol, viniferins and pterostilbene on *Plasmopara viticola* zoospore mobility and disease development. *Vitis, 43*. doi:10.5073/vitis.2004.43.145-148

Pezet, R., Perret, C., Jean-Denis, J. B., Tabacchi, R., Gindro, K., & Viret, O. (2003). δ-viniferin, a resveratrol dehydrodimer: one of the major stilbenes synthesized by stressed grapevine leaves. *Journal of Agricultural and Food Chemistry, 51*(18), 5488-5492. doi:10.1021/jf030227o

Richard, T., Abdelli-Belhad, A., Vitrac, X., Waffo-Teguo, P., & Mérillon, J.-M. (2016). *Vitis vinifera* canes, a source of stilbenoids against downy mildew. *OENO One, 50*(3), 137-143. doi:10.20870/oeno-one.2016.50.4.1178

Rivière, C., Pawlus, A. D., & Mérillon, J. M. (2012). Natural stilbenoids: distribution in the plant kingdom and chemotaxonomic interest in Vitaceae. *Natural Product Reports, 29*(11), 1317-1333. doi:10.1039/C2NP20049J

Romain, C., Bresciani, L., Gaillet, S., Feillet-Coudray, C., Calani, L., Bonafos, B., Vidé, J., Rugani, N., Ramos, J., Rio, D. D., Cristol, J.-P., & Rouanet, J.-M. (2014). Moderate chronic administration of Vineatrol-enriched red wines improves metabolic, oxidative, and inflammatory markers in hamsters fed a high-fat diet. *Molecular Nutrition & Food Research, 58*(6), 1212-1225. doi:10.1002/mnfr.201300853

Sako, M., Hosokawa, H., Ito, T., & Iinuma, M. (2004). Regioselective oxidative coupling of 4-hydroxystilbenes: synthesis of resveratrol and ε-viniferin (E)-dehydrodimers. *Journal of Organic Chemistry, 69*(7), 2598-2600. doi:10.1021/jo035791c

Schnee, S., Queiroz, E. F., Voinesco, F., Marcourt, L., Dubuis, P. H., Wolfender, J. L., & Gindro, K. (2013). *Vitis vinifera* canes, a new source of antifungal compounds against *Plasmopara viticola*, *Erysiphe necator*, and *Botrytis cinerea*. *Journal of Agricultural and Food Chemistry, 61*(23), 5459-5467. doi:10.1021/jf4010252

Snyder, S. A., Gollner, A., & Chiriac, M. I. (2011). Regioselective reactions for programmable resveratrol oligomer synthesis. *Nature, 474*, 461. doi:10.1038/nature10197

Takaya, Y., Terashima, K., Ito, J., He, Y.-H., Tateoka, M., Yamaguchi, N., & Niwa, M. (2005). Biomimic transformation of resveratrol. *Tetrahedron, 61*(43), 10285-10290. doi:10.1016/j.tet.2005.08.023

Takaya, Y., Yan, K.-X., Terashima, K., Ito, J., & Niwa, M. (2002a). Chemical determination of the absolute structures of resveratrol dimers, ampelopsins A, B, D and F. *Tetrahedron, 58*(36), 7259-7265. doi:10.1016/S0040-4020(02)00785-8

Takaya, Y., Yan, K. X., Terashima, K., He, Y. H., & Niwa, M. (2002b). Biogenetic reactions on stilbenetetramers from Vitaceaeous plants. *Tetrahedron, 58*(45), 9265-9271. doi:10.1016/S0040-4020(02)01191-2

Velu, S. S., Buniyamin, I., Ching, L. K., Feroz, F., Noorbatcha, I., Gee, L. C., Awang, K., Wahab, I. A., & Weber, J.-F. F. (2008). Regio- and stereoselective biomimetic synthesis of oligostilbenoid dimers from resveratrol analogues: influence of the solvent, oxidant, and substitution. *Chemistry--A European Journal, 14*(36), 11376-11384. doi:10.1002/chem.200801575

Vrhovsek, U., Malacarne, G., Masuero, D., Zulini, L., Guella, G., Stefanini, M., Velasco, R., & Mattivi, F. (2012). Profiling and accurate quantification of trans-resveratrol, trans-piceid, trans-pterostilbene and 11 viniferins induced by *Plasmopara viticola* in partially resistant grapevine leaves. *Australian Journal of Grape and Wine Research, 18*(1), 11-19. doi:10.1111/j.1755-0238.2011.00163.x

Wilkens, A., Paulsen, J., Wray, V., & Winterhalter, P. (2010). Structures of Two Novel Trimeric Stilbenes Obtained by Horseradish Peroxidase Catalyzed Biotransformation of trans-Resveratrol and (−)-ε-Viniferin. *Journal of Agricultural and Food Chemistry, 58*(11), 6754-6761. doi:10.1021/jf100606p